Journal of Enhanced Heat Transfer, 16(2) 189–203 (2009)
Reprints available directly from the publisher.
Photocopying permitted by license only.

Heat Transfer in High-Pressure Metal Hydride Systems

KYLE C. SMITH[1*], YUAN ZHENG[1], TIMOTHY S. FISHER[1],

TIMOTHÉE L. POURPOINT[2], & ISSAM MUDAWAR[1]

[1]Mechanical Engineering, Purdue University and [2]Aeronautical and Astronautical Engineering, Purdue University

High-pressure metal hydride vehicular hydrogen storage systems can offer good overall gravimetric and volumetric hydrogen densities. Enhanced heat transfer techniques will be essential to achieve established goals for tank filling times. A numerical model is developed to simulate the hydrogen filling process of a subscale high-pressure metal hydride ($Ti_{1.1}CrMn$) system. The model is validated by comparison of simulated and experimental transient temperature profiles of both metal hydride and gas. The substantial influence of free convection in the system was discovered. As such, heat transfer enhancement by free convection is discussed and illustrated in a practical configuration.

Key words: hydrogen storage; metal hydride; simulation; titanium chromium manganese

*Corresponding author: K. C. Smith, kcsmith@purdue.edu

NOMENCLATURE

A	area, m^2	U	heat transfer coefficient, $W/m^2 \cdot K$
a	Redlich–Kwong constant, $kJ^2 \cdot K^{0.5}/kg^2 \cdot bar$	u	internal energy, kJ/kg
b	Redlich–Kwong constant, m^3/kg	$\overline{u}$	average velocity, m/s
Bi	Biot number, dimensionless	V	volume, m^3
C_a	kinetic rate constant, s^{-1}	v	specific volume, m^3/kg
c	volumetric specific heat, kJ/kg·K	x	ratio of hydrogen to metal atoms, dimensionless
D	diameter, m	Z	compressibility factor, dimensionless
E_a	activation energy, $kJ/kg \cdot H_2$	**Greek symbols**	
F	reaction progress variable, dimensionless	α	thermal diffusivity, m^2/s
Gr	Grashof number, dimensionless	β	coefficient of expansion, K^{-1}
g	gravitational acceleration, m/s^2	Δ	change in a quantity, dimensionless
h	enthalpy, kJ/kg	ΔH_r	heat of reaction, $kJ/kmol \cdot H_2$
K	chemical equilibrium constant, dimensionless	μ	dynamic viscosity, $N \cdot s/m^2$
k	thermal conductivity, W/m·K	ν	kinematic viscosity, m^2/s
L	cylinder length, m	**Subscripts**	
l_c	characteristic length, m	a	array
MW	molar mass, kg/kmol	c	critical
m	mass, kg	eff	effective
Nu	Nusselt number, dimensionless	eq	equilibrium
Pr	Prandtl number, dimensionless	H_2	hydrogen gas
p	pressure, bars	i	inside
p_0	equilibrium standard pressure, bars	j	component j
Q	heat, kJ	jk	heat or mass transfer from component j to k
R	hydrogen gas constant, kJ/kg·K	M	metal
r	radius, m	max	maximum
Ra	Rayleigh number, dimensionless	MH	metal hydride
Re	Reynolds number, dimensionless	o	outside
T	temperature, K	p	pseudo
T_0	equilibrium standard temperature, K	s	surface
t	time, s	**Superscript**	
		i	initial

1. INTRODUCTION

Hydrogen has been suggested by many for use as a fuel replacement in vehicle applications primarily for its substantial environmental benefits. If used to supply a fuel cell, a hydrogen-powered system emits only water vapor. If an environmentally benign energy source is used to generate hydrogen, then its closed-loop emission footprint is zero. Even in the case that hydrogen is produced from a fossil fuel, carbon capture and sequestration technology could be used to eliminate carbon emission in large-scale hydrogen generation [Herzog et al., 2001]. Different types of fuel cells are being developed, and electrical drive trains are well developed, but the storage problem has yet to be solved.

The most conventional and simple way to store hydrogen is as a compressed gas. Because of hydrogen's low molecular weight, it exerts more pressure per unit mass than other gases and thus must be stored at high pressure in a compact system. High-pressure storage requires significant compression energy, and the high-

strength vessels required to withstand the pressure add volume and cost to the vehicle. Liquid storage is another option because of its high mass density of hydrogen, but hydrogen is rapidly lost by evaporation. Also the significant amount of energy required to liquefy hydrogen gas decreases overall efficiency [Zhang et al., 2005]. Other options utilize chemical bonding to store hydrogen at lower pressures and in a more stable state. Different classes of chemical storage include chemical hydrides, hydrogenated compounds, and metal hydrides.

Metal hydrides enable high volumetric storage density of hydrogen by storing it in the solid state. Metal hydrides form by chemical reaction of hydrogen gas with a suitable metal and are useful in fuel cell vehicles because the reaction can be easily reversed. Reversibility of the reaction allows the metal hydride to release hydrogen for fuel cell power generation and then to be replenished with fresh hydrogen. Thus, recharging of fuel and operating the vehicle would be very similar to current gasoline vehicles, easing the transition from fossil fuels to hydrogen.

In metal hydrides, hydrogen forms weak chemisorbed bonds in the interstitial sites of the host metal lattice, causing expansion of the lattice by 20–30% by volume [Schlapbach et al., 1992]. The reversibility of the exothermic hydriding reaction is described by the heat of reaction, ΔH_r. For typical metal hydrides, the reaction heating is ten times larger than compression heating and thus requires enhanced heat transfer during the hydriding process [Zheng et al., 2006]. Efficient dissipation of this energy is also important to satisfy the overall efficiency of the vehicle.

To operate vehicles and sustain an economy with this storage technology gaseous hydrogen would be delivered to filling stations. On-board vehicle tanks would be manufactured to contain metal hydride powders or compacts, and hydrogen filling would occur at a station. After filling, hydrogen gas would be drawn from the metal hydride at the demands of the fuel cell. After hydrogen is depleted from the metal hydride, vehicles would return to the filling station to replenish with hydrogen gas. Customers will also require a fast hydrogen filling process, comparable to gasoline fill times of one to several minutes.

Intermetallic metal hydride systems have been used extensively in the past for different applications including hydrogen storage, adsorption heat pumps, and battery technology [Sastri et al., 1998]. Further, many new complex metal hydrides are being developed but have not been studied in real applications [Jorgensen, 2007]. Hydrides have the potential to achieve both high gravimetric and volumetric storage densities of hydrogen when combined in a hybrid tank containing high-pressure hydrogen [Takeichi et al., 2003]. These possibilities make high-pressure metal hydrides systems closest to near-term commercialization in vehicles than low-pressure hydrides [Jorgensen, 2007].

The specific metal studied herein is $Ti_{1.1}CrMn$, which forms a high-pressure metal hydride at a dissociation pressure greater than 100 bars at 296 K [Kojima et al., 2006]. Equilibrium properties for TiCrMn hydrides have been studied [Beeri et al., 2000]. Some thermo-chemical properties of the class of materials $Ti_xCr_{2-y}Mn_y$ ($0.96 \le x \le 1.41$, $0.09 \le y \le 1.66$) were studied [Kojima et al., 2006], but detailed kinetic characteristics for these alloys are not readily available in the literature.

Modeling and simulation are very important in understanding and analyzing metal hydride hydrogen storage systems, particularly when the system cannot be instrumented to measure every aspect of the filling and release processes. Simulation can also guide improvements in system performance. Motivated by this, the specific objectives of this study are as follows:

- To develop a numerical model that captures major physical and chemical processes in a subscale high-pressure metal hydrogen (HPMH) hydrogen storage system.
- To simulate the hydrogen filling process in a subscale HPMH vessel with different pressurization and cooling schemes.
- To understand the effects of different heat transfer mechanisms on the filling process so that future containment and cooling systems might be designed to provide higher capacity and more rapid filling.

2. HEAT AND MASS TRANSFER MODELING

Modeling of heat and mass transfer in high-pressure metal hydrides, hydrogen gas, and real engineering systems requires a comprehensive approach to account for the interactions among the system components, high-pressure gas, and the reacting chemical species. A summary of the metal hydrides previously modeled and typical hydriding pressures and temperatures is listed in Table 1. Previous work in the area of metal

TABLE 1. Previous Heat and Mass Transfer Modeling of Metal Hydride Systems

Hydrogen storage alloy	p_{eq}, bars	T_{eq}, °C	References	
			Model	Data
$LaNi_5$	1.6	25	[Kumar Phate et al., 2007; Marty et al., 2006; MacDonald & Rowe, 2006; Askri et al., 2004a,b; Kaplan & Veziroglu, 2003; Aldas et al., 2002; Mat et al., 2002; Nakagawa et al., 2000; Jemni & Ben Nasrallah, 1995; El-Osairy et al., 1993; Aoki & Mitsui, 1991]	[Kumar Phate et al., 2007]
$LmNi_5$	1.6	10	[Mat et al., 2001; Mayer et al., 1986]	[Mayer et al., 1986]
$LaNi_{4.7}Al_{0.3}$	1	50	[Gopal & Murthy, 1992]	[Nakamura et al., 2000]*
$MINi_{4.5}Mn_{0.5}$	0.3	50	[Sun & Deng, 1989]	[Nakamura et al., 2000]**
$MmNi_{4.5}Al_{0.5}$	5	25	[Gopal & Murthy, 1995]	[Gopal & Murthy, 1995]
$Ti_{0.42}Zr_{0.58}Cr_{0.78}Fe_{0.57}Ni_{0.2}Mn_{0.39}Cu_{0.03}$	10	41	[Oi et al., 2004]	[Oi et al., 2004]
$Ti_{0.98}Zr_{0.02}V_{0.43}Fe_{0.09}Cr_{0.05}Mn_{1.5}$	10	23	[MacDonald & Rowe, 2007]	[MacDonald & Rowe, 2007]
$TiMn_{1.5}$	20	30	[Sun & Deng, 1988]	[Sun & Deng, 1988]
TiCrMn	140	30	[Toh et al., 2006]	[Kojima et al., 2006]

*Equilibrium properties estimates by those of $LaNi_{4.75}Al_{0.25}$
**Equilibrium properties estimates by those of $LaNi_{4.5}Mn_{0.5}$

hydride heat and mass transfer simulations has focused primarily on low-pressure metal hydrides, with LaNi5 hydrides receiving the most attention. Only one thermal model for high-pressure metal hydride systems was found in the literature, and that model was not validated by experiment.

2.1 System Configuration

The system of interest is comprised of a stainless steel tank that contains $Ti_{1.1}CrMn$, a finned heat exchanger, and a filler material, all of which are shown in Figure 1. An experimental pressure vessel was designed in order to allow testing of 1/70th to 1/5th of the scale of a system that would be used in a passenger vehicle. Ballast material made of Huntsman Ren Shape™ 2000 epoxy board was added to the vessel to fill void space, so that the experimental measurements would be more sensitive to the chemical reaction than to compression of the bulk gas.

Hydrogen filling experiments were conducted at the Hydrogen Systems Laboratory, part of the Maurice Zucrow Laboratories at Purdue University. This lab houses two test cells and a control room refurbished and upgraded for hydrogen service compatibility. The laboratory is designed in accordance with NFPA and NASA standards for hydrogen safety. The high pressure, high capacity hydrogen feed system is remotely controlled from a computerized data acquisition and

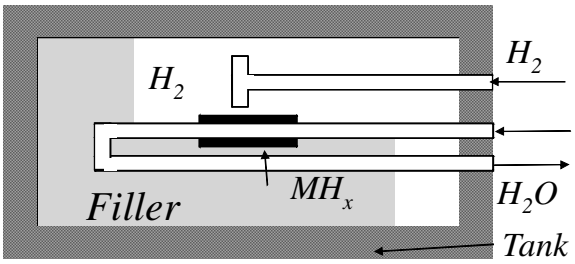

FIGURE 1. Metal hydride test vessel.

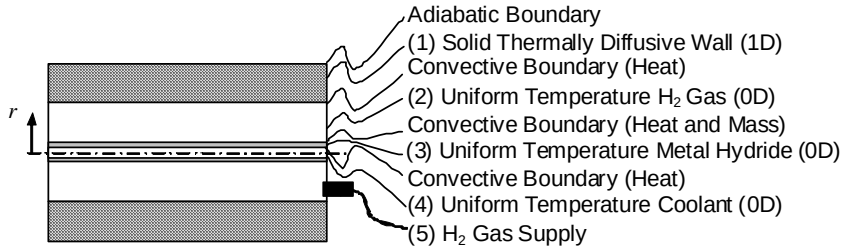

FIGURE 2. Simplified system configuration.

control systems. Testing with high-pressure conventional reversible metal hydrides is performed in this laboratory at pressures up to 330 bars. With a total cooling capacity of 10 kW provided by a Neslab HX-300 DD chiller, the cooling system functions in closed-loop mode and is compatible with standard automotive coolants at flow rates up to 45 liters per minute. Any pressurization profile can be programmed in the data acquisition and control system to mimic a hydrogen filling process of an on-board system at a hydrogen filling station.

All experimental results presented herein were obtained in tests during which the tank pressure was regulated in a linear fashion with respect to time; typically the maximum tank pressure of 280 bars was obtained in three successive linear pressure ramps. This approach allowed for more efficient use of the hydrogen gas supply while allowing for a simplified study of the interactions among heat/mass transfer and mechanical/chemical processes during tank filling. Once the desired maximum pressure was reached, it was regulated to be constant with respect to time. This pressurization sequence was repeated until the final operating pressure of the tank was attained.

Geometric complexity and uncertainty motivated a modeling effort that attempted to capture the basic physical processes in the system. Thus, a simplified mathematical model was developed to consider different levels of dimensionality for each component in the system. As shown in Figure 2, a 1D radial model was employed with each component separated by a convective boundary. Figure 2 displays numbers for each system component that correspond to subscripted variables in the governing equations.

The flow behavior of the hydrogen gas in the experimental system is very complex as hydrogen interacts with the tank wall and the metal hydride. The gas expands at the inlet tube and then compresses in the tank. The geometry of the surrounding solid surfaces induces complex interactions with the fluid. This model treats the bulk gas as having uniform temperature with convective boundaries. This approach allows the dominant mechanisms of convective thermal transport to be modeled in a mathematically simple fashion. Mass is transferred into the chamber from the supply tube, as well as from the bulk gas into the metal as the hydriding process proceeds. Kinetic energies and potential energies are neglected.

2.2 Governing Equations

The mass and energy conservation equations for the bulk gas are

$$\frac{dm_2}{dt} = \dot{m}_{52} - \dot{m}_{23} \tag{1}$$

$$\frac{d\left(m_2 u_2\right)}{dt} = -\dot{Q}_{23} - \dot{Q}_{21} + \dot{m}_{52} h_5 - \dot{m}_{23} h_2 \tag{2}$$

Equations (1) and (2) can be combined to yield

$$m_2 \frac{du_2}{dt} = -\dot{Q}_{23} - \dot{Q}_{21}$$

$$+ \dot{m}_{52}(h_5 - u_2) - \dot{m}_{23}(h_2 - u_2) \tag{3}$$

The mass of the bulk gas is determined from real gas properties [Vargaftik, 1975], the volume of the pressure vessel excluding the solid contents, and lookups for its specific volume, as

$$m_2 = \frac{V_2}{v(p_2, T_2)} \tag{4}$$

Heating and cooling of the metal hydride occur by three mechanisms: convection from the bulk gas, con-

vection to the coolant, and volumetric chemical reaction heating. Also, hydrogen mass is transferred from the bulk gas chemically into the metal to form metal hydride

$$M + \frac{x_{\max}}{2} H_2 \rightarrow MH_{x_{\max}} \tag{5}$$

The hydrogen mass flow rate into the metal hydride is determined by the rate of reaction

$$\dot{m}_{23} = x_{\max} m_M^i \frac{\mathrm{M}_H}{\mathrm{M}_M} \frac{dF}{dt}, \quad F = \frac{x}{x_{\max}} \tag{6}$$

Assuming negligible expansion or compression of the solid metal hydride and constant heat of reaction, energy is conserved as

$$(mc)_{eff} \frac{dT_3}{dt} = \dot{Q}_{32} - \dot{Q}_{34} + \dot{m}_{23} \frac{\Delta H_r}{MW_{H_2}} \tag{7}$$

$$(mc)_{eff} = (m_{3,M} c_M + m_{3,MH} c_{MH}) \tag{8}$$

The effective thermal mass of the metal and its hydride are considered collectively in Eq. (8) due to uncertainty in their properties.

Experimental results indicate that the hydriding reaction is limited by surface dissociation or nucleation and growth of hydride at the surface followed by diffusion limitation for the remainder of the reaction [Asakuma et al., 2003; Han & Lee, 1989]. The rate of nucleation and growth depends on the amount of defects and impurities capable of serving as nucleation sites in the material [Asakuma et al., 2003], whereas surface dissociation rates depend on the activation energy of the surface [Mayer et al., 1986]. The diffusion limitation is neglected in this work, since the concentration at which transition from the initial limiting process to being limited by diffusion is unknown. Also, it is assumed that a sufficient number of nucleation sites exist such that nucleation and growth does not limit the reaction. Thus, the kinetic relation which reflects surface dissociation as the rate limiting step is utilized to model the kinetic behavior of $Ti_{1.1}CrMn$ [Mayer et al., 1986]

$$\frac{dF}{dt} = C_a \exp\left(\frac{-E_a}{RT}\right) \ln\left(\frac{p}{p_{eq}}\right) (1 - F) \tag{9}$$

The kinetic parameters used in the model were C_a = 54.7 s^{-1} and E_a = 20,700 kJ/kmol·H_2 [Zheng et al., 2006]. Equilibrium behavior of metal hydrides is represented by pressure composition isotherms, which can be estimated by the Van't Hoff equation of chemical equilibrium [Çengal & Boles, 2002]

$$\ln\left(\frac{K_{p0}}{K_{p_{eq}}}\right) = \frac{\Delta H_r}{R}\left(\frac{1}{T} - \frac{1}{T_0}\right) \tag{10}$$

A major assumption of this relation is that the heat of reaction does not vary with temperature [Çengal & Boles, 2002]. For a real gas, the ratio of equilibrium constants is expressed as the inverse ratio of fugacities. In this work, the real gas effect of fugacity is not included since detailed pressure-composition isotherms for this material are not available

$$\frac{K_{p0}}{K_{p_{eq}}} = \frac{P_{eq}}{p_0} \tag{11}$$

For this model, it is assumed that ΔH_r = –22,000 kJ/kmol·H_2, T_0 = 194.0 K, and p_0 = 1 atm [Kojima et al., 2006]. Note that these parameters are assumed to be constant, though real materials exhibit some variation with composition [Fukai, 2005]. A detailed investigation of the thermo-chemical behavior will be undertaken in future work.

The solid tank wall was considered to be thermally diffusive, having temperature which varies radially as heat diffuses through it. A more conductive material could possibly have been treated as a lumped mass. This effect could be assessed by evaluating the Biot number, Bi = Ul_c/k. Thermal gradients in the solid should be considered when the Biot number exceeds 0.1 [Incropera et al., 2007]. For the geometry of interest, the Biot number ranges from about 1 to 10; thus, gradients must be considered.

The thermal behavior of low-conductivity materials is governed by the heat diffusion equation. Heat transfer at the outside tank wall is considered negligible; at the inner wall heat is transferred by convection

$$\frac{1}{\alpha}\frac{\partial T_1}{\partial t} = \frac{1}{r}\frac{\partial}{\partial r}\left(r\frac{\partial T_1}{\partial r}\right) \tag{12}$$

$$kA_o \left.\frac{\partial T_1}{\partial r}\right|_{r=r_o} = 0 \tag{13}$$

$$kA_i \left.\frac{\partial T_1}{\partial r}\right|_{r=r_i} = -\dot{Q}_{12} \tag{14}$$

Likewise, temperature gradients in the metal hydride are neglected in this analysis because the related Biot numbers are of the order of 0.1.

2.3 Real Gas Behavior

Gases behave in a nearly ideal sense at low pressures and high temperatures. Pressures encountered in hydrogen storage are often higher and temperatures are lower than those that are appropriate for hydrogen to be considered an ideal gas. Thus, there is a need to evaluate equilibrium thermodynamic states of the real gas. Different equations of state were surveyed and compared to real gas data; the result is shown in Figure 3. The Redlich–Kwong equation [Moran & Shapiro, 2004] fits well and is expressed simply in equation form:

$$p = \frac{RT}{v-b} - \frac{a}{\sqrt{T}v(v+b)} \tag{15}$$

$$a = p_c^{-1}0.42748R^2T_c^{2.5}, \quad b = p_c^{-1}0.08662RT_c$$

Another implication of real gases is that thermodynamic properties depend on compressibility. For instance, the change in specific internal energy is expressed with Maxwell's relations for a real gas. The term that depends on compressibility drops out for ideal gases, but must be considered for non-ideal gases

$$du = c_v dT + \left\{ T\left(\frac{dp}{dT}\right)_v - p \right\} dv \tag{16}$$

The bracketed term preceding d_v in Eq. (16) represents a residual pressure that acts to increase internal energy as expansion occurs (positive d_v). Physically, it is a consequence of increasing repulsive forces between gas molecules as pressure increases. This quantity is referred to as a 'pseudo-pressure' in this analysis. For the Redlich–Kwong, this term simplifies to

$$p_p = \frac{1.5a}{\sqrt{T}v(v+b)} \tag{17}$$

As shown in Figure 4, the pseudo-pressure increases with pressure and decreases with temperature. These trends are expected considering that gases are nearly ideal (Z = 1, p_p = 0) at low pressure and high temperature. The following equation thus represents the differential change in internal energy due to temperature and volume changes

$$du = c_v dT + \frac{1.5a}{\sqrt{T}v(v+b)} dv \tag{18}$$

After integration of Eq. (18), the isothermal change in internal energy is expressed as

$$u_2 - u_1 = \frac{1.5a}{b\sqrt{T_1}} \ln\left(\frac{v_2(v_1+b)}{v_1(v_2+b)}\right) \tag{19}$$

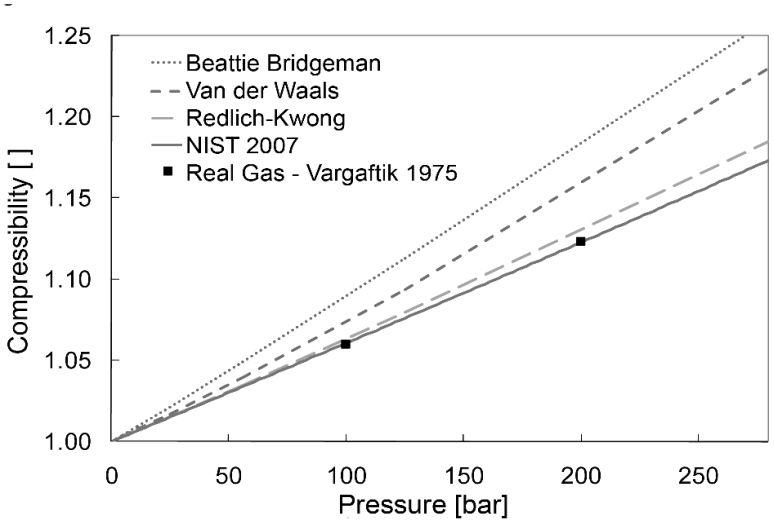

FIGURE 3. H_2 compressibility factor for various state equations at 300 K.

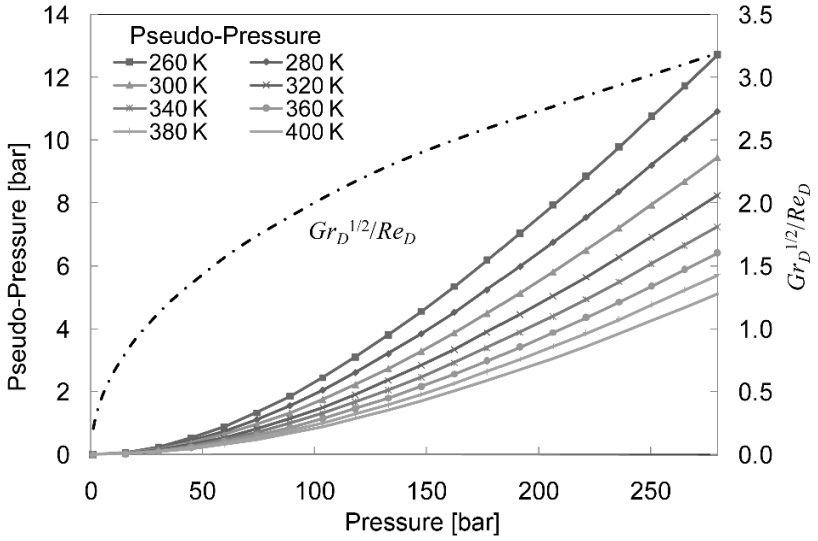

FIGURE 4. Pseudo-pressure as a function of pressure.

The significance of this non-ideal effect is best illustrated with thermodynamic processes. Isothermal compression from 1 to 280 bars would decrease the hydrogen's internal energy by 53.7 kJ/kg; for hydrogen as an ideal gas with this change in energy, the temperature would decrease by 5°C. Since heat transfer rates between the gas and metal hydride depend on temperature, a 5°C difference has a significant impact on the simulated results.

2.4 Convective Heat Transfer Terms

Coolant is capable of passing through the tube in the center of the tank, but the experimental conditions presented here had no coolant flow, meaning effectively that $\dot{Q}_{34} = 0$. The convective boundaries of hydrogen gas with the tank wall and the metal hydride must be considered, however. Many who have studied hydrogen storage in the high-pressure compressed gaseous state have employed three-dimensional thermal-fluid models due to the coupled behavior of free convection, forced convection, and unsteady compression [Itoh et al., 2007]. Simplifying thermal and flow gradients into a convective boundary significantly reduces analytical complexity. Here, contributions from the two convection modes are addressed separately assuming quasi-steady compression.

The relative influence of free and forced convection can be assessed by comparing their respective driving forces. For forced convection the Reynolds number is a measure of inertia to viscous forces. Assuming that momentum is transferred primarily in the axial direction of tank, the appropriate Reynolds number is

$$Re_D = \frac{4\dot{m}}{\pi D \nu \rho} \tag{20}$$

The alternative convection mode, free convection, is caused by buoyancy forces inducing fluid circulation in the cylinder. As hot fluid is cooled by the surface at the top of the cylinder, the fluid's density decreases and it falls along the cylinder wall due to gravity. While falling to the bottom, heat is transferred to the fluid decreasing its density eventually causing it to rise in the center of the tank; the flow pattern reaches steady state in a finite amount of time. To quantify the extent to which the fluid is influenced by free convection the Grashof number is considered

$$Gr_D = \frac{g\beta(T - T_s)D^3}{\nu^2} \tag{21}$$

When formulating momentum and energy equations for free convection problems, it can be shown that the Grashof number represents the square of an equivalent Reynolds number for the forced convection problem [Incropera et al., 2007]. Thus, a measure of buoyancy to inertial forces of a system with free and forced convection can be determined by $\mathrm{Gr}_D^{1/2}/\mathrm{Re}_D$

$$\frac{Gr_D^{1/2}}{\mathrm{Re}_D} = \frac{\pi D^2 \rho \sqrt{g\beta(T - T_s)}}{4\dot{m}} \tag{22}$$

Tank diameters in hydrogen storage systems often have very large diameter and density is large particularly for high-pressure metal hydride systems. Also, it is expected that a large temperature difference will exist between the tank and the gas inside, as has been shown numerically and experimentally [Itoh et al., 2007]. Equation (22) indicates that free convection will increase with each of the aforementioned parameters, making it a significant thermal aspect to be modeling. Free convection is inversely proportional to the mass flow rate, which is expected to be small even for fast filling of tanks. Equation (22) was evaluated for a 34L cylindrical tank 200 mm in diameter, similar to the Type 3 composite tank described in the literature [Itoh et al., 2007]. Mass flow rate was chosen to achieve fast filling of the tank (1 to 350 bar in 90 s) in order to simulate the maximum rate of forced convection. Gas and wall temperatures of 320 K and 300 K respectively used in the calculation were chosen to represent typical thermal conditions. The result shown in Figure 4 indicates that free convection is significant for the high-pressure range. In the system of interest temperature differences and pressures are large, and the flow rate is moderate. Consequently, heat transfer from the bulk gas is modeled by free convection, based on the results presented. In particular, Kuehn and Goldstein developed Nusselt number correlations for internal free convection of fluid in horizontal cylinders and for an inner concentric horizontal cylinder [Kuehn & Goldstein, 1976], which are both valid for stagnant, laminar, and turbulent flow regimes. The resulting rates of heat transfer from the gas to the solid wall and the metal hydride depend on these Nusselt numbers as follows:

$$Nu_{D_o} = \frac{-2}{\ln\left(1-2\left(\left[\left(\frac{1}{1-e^{-0.25}}\right)^{\frac{5}{3}}+0.587Ra_{D_o}{}^{\frac{5}{12}}\right]^{9}+0.1Ra_{D_o}{}^{5}\right)^{\frac{-1}{15}}\right)} \tag{23}$$

$$Nu_{D_i} = \frac{2}{\ln\left(1+2\left(0.518Ra_{D_i}{}^{\frac{15}{4}}\left(1+\left(\frac{0.559}{Pr}\right)^{\frac{3}{5}}\right)^{\frac{-25}{4}}+0.1Ra_{D_i}{}^{5}\right)^{-\frac{1}{15}}\right)} \tag{24}$$

$$\dot{Q}_{32} = k_{H_2} Nu_{D_o} \pi L (T_3 - T_2) \tag{25}$$

$$\dot{Q}_{21} = k_{H_2} Nu_{D_i} \pi L (T_2 - T_1) \tag{26}$$

2.5 Numerical Methods

Temperature terms in the governing equations were discretized by the finite difference method in time and the explicit finite volume method in space. Reaction progress was calculated by numerical integration of the reaction progress rate. The numerical time step was set to be smaller than the sampling frequency of experimental pressure data. Spatial cell size of the tank wall was reduced until the difference in temperature was less than 10^{-5} °C with the addition of another cell. The time step was checked to be sufficiently small to ensure stability for the cell size

$$\Delta t < (\Delta r)^2 / 2\alpha \tag{27}$$

Chemical and convective terms were highly nonlinear with respect to temperature. It was necessary to supply a guess at each time step in order to evaluate chemical and convective terms. The subsequent temperature solution was then substituted for the original guess from which chemical and convective terms were evaluated. This iteration process repeated until convergence between guessed and solved temperatures was reached within 10^{-5} °C.

3. RESULTS AND DISCUSSION

3.1 Simulated and Experimental Results

Simulations and experiments were performed in order to validate the modeling work with unactivated metal hydride meaning it has not been prepared to chemically react. In Figure 5, experimental temperatures are compared to simulated temperatures for the bulk hydrogen and metal hydride. The temperature changes due to pressurization agree within 20% of the experimental values. The simulated temperatures differ from experimental partly because of the lumped hydrogen gas assumption. In fact temperature gradients must be present in the gas in order for natural convection to occur. Temperature sensors in the experiment were closer to the metal hydride boundary, thus measuring a temperature closer to that of the metal hydride. Also, with forced convection present during the pressurization the simulated peak temperatures were lower. The peak temperature agrees better as pressure increases,

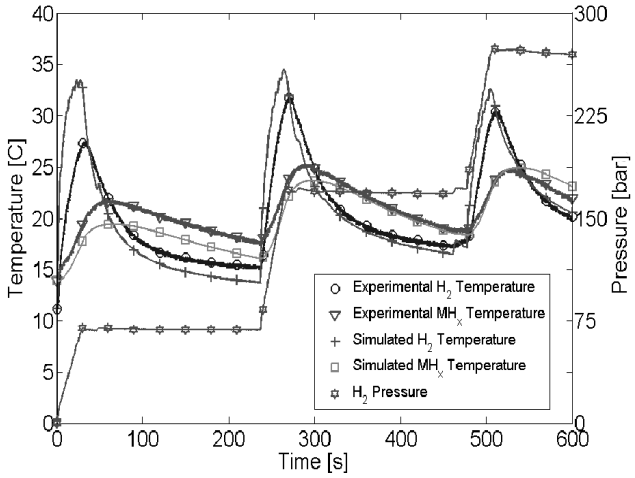

FIGURE 5. Experimental and simulated temperatures for a test with unactivated metal hydride and no coolant flow.

because the influence of free convection becomes greater.

The temperature decay rates are well described by the model; this decay rate depends directly on the ratio of convection to thermal mass. This result implies that the rate of change of the average hydrogen temperature is well described. Note that during the time at which the temperature decay occurs forced convection is negligible. Thus, the matching decay rate implies that the free convection model for the bulk gas fits well in this pressurization regime.

The hydriding reaction adds significant complexity to the model, because large uncertainties are associated with the equilibrium and kinetic behaviors of the metal hydride. To limit contamination and increase safety during preparation of the metal hydride, a special containment vessel was designed to isolate the material from oxidation agents. Its thermal mass was lumped into the hydrogen thermal mass in this model.

The activated metal hydride was pressurized and the results are shown in Figure 6. Temperature and pressure were measured during the experiment, and comparison to the model provides insight into heat transfer and the metal hydride reaction. The results for temperature rise and decay times agree very well, with the exception of the pressure step to 100 bars. At that

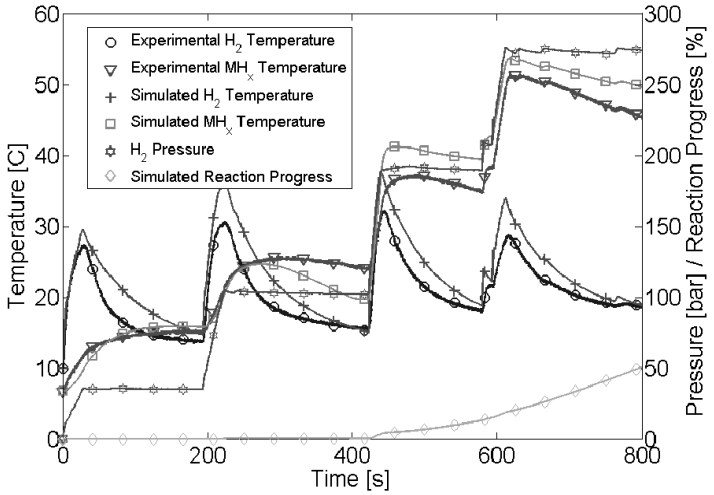

FIGURE 6. Experimental and simulated results for a test with activated metal hydride and no coolant flow.

particular pressure step very little temperature decay was observed in the metal hydride, whereas it was simulated to be much greater. This effect occurred because the experimental chemical reaction actually began before the simulated reaction, suggesting that the equilibrium pressure for that temperature is actually lower than what was used in the simulation. This error could be corrected by using more accurate values for ΔH_r and T_0 determined by pressure composition isotherm measurements of the metal hydride reaction.

3.2 Heat Transfer Enhancement

High-pressure metal hydrides have volumetric storage densities which are sufficient to meet DoE targets for hydrogen storage, but their gravimetric densities are too low. Takeichi et al. have shown that hybrid gaseous hydrogen/metal hydride storage systems could provide reasonable gravimetric density while compromising volumetric density [Takeichi et al., 2003]. The hybrid system proposed would contain a small amount of metal hydride with the remainder of the tank volume occupied by gaseous hydrogen, roughly resembling the system modeled in this work. Since it was concluded that free convection has significant cooling capacity and that hybrid systems have promise for storage applications, engineering designs should be optimized to enhance heat transfer by free convection.

To enhance heat transfer the metal hydride could be distributed throughout the tank by increasing heat transfer area and local heat transfer coefficient. To quantify this effect heat transfer is considered from some fixed volume fraction of metal hydride distributed in the form of N cylinders inside a cylindrical tank. Each cylinder in the arrangement is considered to have the same temperature while bulk gas around the cylinders is at uniform temperature. Kuehn and Goldstein [1976] suggest a correlation for heat transfer from an array of cylinders to surrounding bulk fluid inside another cylinder

$$Nu_{D_i,a} = \frac{2N}{\ln\left(1 + 2/Nu_{D_i}\right) - N \ln\left(1 - 2/Nu_{D_a}\right)} \quad (27)$$

under the assumptions that (1) inner cylinders are at a common temperature and (2) the bulk fluid has a uniform temperature. Heat transfer from only a small number of cylinders (<5) was studied in order to reasonably satisfy assumptions. For a 34L cylindrical tank 200 mm in diameter heat transfer from cylinders at 350 K to bulk hydrogen at 280 bars and 300 K was calculated. The resulting heat transfer rates and surface areas were then normalized by the values for a single cylinder.

For the results shown in Figure 8, cylinders filled 25% of the space in the outer cylinder, leaving 75% for the bulk gas. As shown by the results, distributing the metal hydride into one cylinder provides dramatic heat transfer enhancement over the undistributed configuration. Even more, the result suggests that splitting the material into smaller cylinders enhances free convection further. Heat transfer enhancement scales in a nearly linear fashion with respect to the number cylinders. In reality the heat transfer rate would decrease after some number of cylinders due to large temperature gradients in the bulk gas. To consider the effect of conduction direct three-dimensional simulation of the buoyant flow would be necessary.

The strong dependence of free convection on pressure of the convective fluid was discussed in section 2.4. Accordingly, a range of pressures exists for which free convective cooling will be adequate. For this reason volumetric heat dissipation rates were calculated as a function of pressure for 5 configurations of distributed hydride, as shown in Figure 9. A metal hydride with density of 7 g/cc, 2 wt. % hydrogen, and ΔH_r = –22,000 kJ/kmol·H_2 would require an average volumetric heat dissipation of 2.2 MW/m^3 in order to completely react in 5 minutes. Considering this, free convective enhancement would be inadequate at low pressures but would be sufficient at higher pressures.

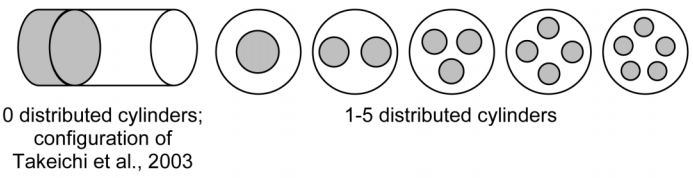

FIGURE 7. Metal hydride arrangements for 25% volume fraction. Metal hydride cylinders are represented by gray circles.

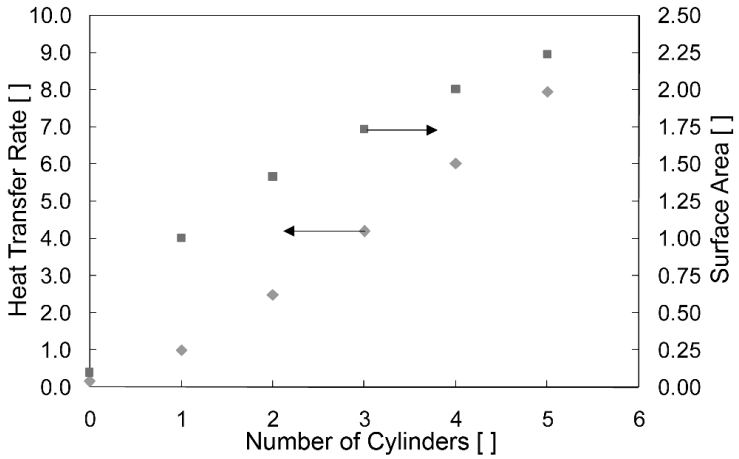

FIGURE 8. Normalized heat transfer and surface area for arrays of cylinders with 25% hydride volume fraction. The data for zero cylinders correspond to the metal hydride configuration in [Takeichi et al., 2003] based on vertical plate correlations for free convection [Incropera et al., 2007].

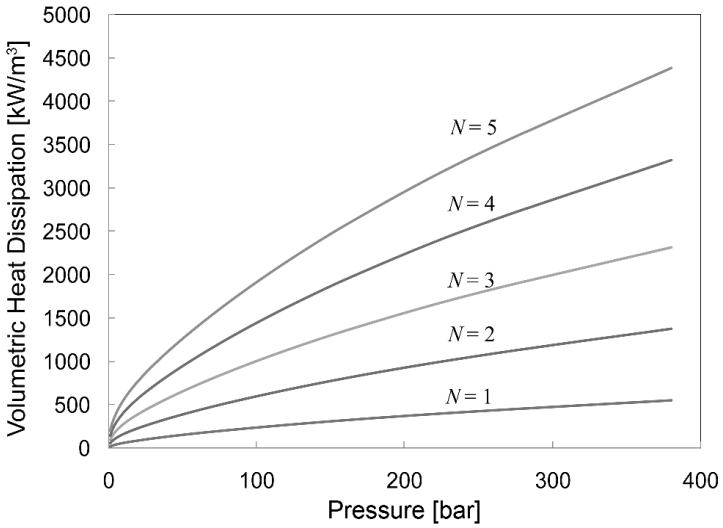

FIGURE 9. Volumetric heat dissipation by free convection as a function of pressure for ΔT = 50 K with 25% hydride volume fraction.

CONCLUSIONS

A transient numerical model was developed to simulate the hydrogen filling process in a subscale HPMH vessel. Hydrogen bulk gas and metal hydride inside the vessel were thermally lumped at two different temperatures and the vessel wall was treated as a one-dimensional thermally diffusive boundary. The simulated transient temperature profiles of the metal hydride and compressed hydrogen matched experimental data reasonably well. The applied correlations for convection represent the heat transfer to and from the gaseous phase very well. The quasi-static assumption of the filling process is valid for this system. Real and idealized behaviors of hydrogen gas were compared, and the real gas properties were shown to model the gas

phase accurately. It was discovered that free convection in the bulk compressed hydrogen space is a very important heat transfer mode in subscale HPMH hydrogen storage systems and could be utilized to enhance heat transfer in hybrid systems.

Potential areas of improvement to the model include spatial variation of temperature in the metal hydride, forced convection from hydrogen gas, and more accurate sub-models for thermo-chemical and kinetic behavior of the metal hydride. These are topics of ongoing studies.

ACKNOWLEDGMENTS

The authors thank General Motors for its sponsorship of the experimental work contained herein. The lead author wishes to thank the National Science Foundation for its financial support through a graduate research fellowship. Any opinions, findings, conclusions or recommendations expressed in this publication are those of the authors and do not necessarily reflect the views of the National Science Foundation.

REFERENCES

Aldas, K., Mat, M. D., and Kaplan, Y. (2002) A Three-Dimensional Mathematical Model for Absorption in a Metal Hydride Bed, *Int. J. Hydrogen Energy*, Vol. 27, Issue 10, pp. 1049–1056.

Aoki, H. and Mitsui, H. (1991) Tubular Heat Exchangers with Internal Longitudinal Fins for Metal Hydride Reaction Beds, Nippon Kikai Gakkai Ronbunshu, *B Hen/Trans. JSME, Part B*, Vol. 57, Issue 534, pp. 604–608.

Asakuma, Y., Miyauchi, S., Yamamoto, T., Aoki, H., and Miura, T. (2003) Numerical Analysis of Absorbing and Desorbing Mechanism for the Metal Hydride by Homogenization Method, *Int. J. Hydrogen Energy*, Vol. 28, Issue 5, pp. 529–536.

Askri, F., Jemni, A., and Ben Nasrallah, S. (2004a) Dynamic Behavior of Metal–Hydrogen Reactor during Hydriding Process, *Int. J. Hydrogen Energy*, Vol. 29, Issue 6, pp. 635–647.

Askri, F., Jemni, A., and Ben Nasrallah, S. (2004b) Prediction of Transient Heat and Mass Transfer in a Closed Metal–Hydrogen Reactor, *Int. J. Hydrogen Energy*, Vol. 29, Issue 2, pp. 195–208.

Beeri, O., Cohen, D., Gavra, Z., Johnson, J. R., and Mintz, M. H. (2000) Thermodynamic Characterization and Statistical Thermodynamics of the TiCrMn-H2(D2) System, *J. Alloys Compounds*, Vol. 299, Issue 1–2, pp. 217–226.

Çengal, Y. A. and Boles, M. A. (2002) *Thermodynamics: An Engineering Approach*, 4th ed., McGraw-Hill, New York.

El-Osairy, M. A., El-Osery, I. A., Metwally, A. M., and Hassan, M. A. (1993) Two-Dimensional Dynamic Analysis of Metal Hydride Hydrogen Energy Storage Conduction Bed Models, *Int. J. Hydrogen Energy*, Vol. 18, Issue 6, pp. 517–524.

Fukai, Y. (2005) *The Metal–Hydrogen System: Basic Bulk Properties*, 2nd ed., Springer, Berlin.

Gopal, R. M. and Murthy, S. S. (1992) Prediction of Heat and Mass Transfer in Annular Cylindrical Metal Hydride Beds, *Int. J. Hydrogen Energy*, Vol. 17, pp. 795–805.

Gopal, R. M. and Murthy, S. S. (1995) Studies on Heat and Mass Transfer in Metal Hydride Beds, *Int. J. Hydrogen Energy*, Vol. 20, Issue 11, pp. 911–917.

Han, J. I. and Lee, J. (1989) Hydriding Kinetics of LaNi5 and LaNi4.7Al0.3, *Int. J. Hydrogen Energy*, Vol. 14, Issue 3, pp. 181–186.

Herzog, H. J. (2001) What Future for Carbon Capture and Sequestration? *Environ. Sci. Technol.*, Vol. 35, Issue 7, pp. 148A–153A.

Incropera, F. P., Dewitt, D. P., Bergman, T. L., and Lavine, A. S. (2007) *Fundamentals of Heat and Mass Transfer*, 6th ed., John Wiley & Sons, Hoboken, NJ.

Itoh, Y., Tamura, Y., Mitsuishi, H., and Watanabe, S. (2007) Numerical Study of the Thermal Behavior on Fast Filling of Compressed Gaseous Hydrogen Tanks. SAE Technical Paper Series: 2007 World Congress, Detroit, Michigan.

Jemni, A. and Ben Nasrallah, S. (1995) Study of Two-Dimensional Heat and Mass Transfer during Absorption in a Metal-Hydrogen Reactor, I*nt. J. Hydrogen Energy*, Vol. 20, Issue 1, pp. 43–52.

Jorgensen, S. (2007) Engineering Hydrogen Storage Systems, *Proc. 2nd Energy Nanotechnology Int. Conf.*, September 5–7, 2007, Santa Clara, CA, pp. 19–20.

Kaplan, Y. and Veziroglu, T. N. (2003) Mathematical Modeling of Hydrogen Storage in a LaNi5 Hydride Bed, *Int. J. Energy Res.*, Vol. 27, Issue 11, pp. 1027–1038.

Kojima, Y., Kawai, Y., Towata, S., Matsunaga, T., Shinozawa, T., and Kimbara, M. (2006) Development of Metal Hydride with High Dissociation Pressure, *J. Alloys Compounds*, Vol. 419, Issue 1–2, pp. 256–261.

Kuehn, T. H. and Goldstein, R. J. (1976) Correlating Equations for Natural Convection Heat Transfer between Horizontal Circular Cylinders, *Int. J. Heat Mass Transfer*, Vol. 19, pp. 1127–1134.

Kumar Phate, A., Prakash Maiya, M., and Murthy, S. S. (2007) Simulation of Transient Heat and Mass Transfer during Hydrogen Sorption in Cylindrical Metal Hydride Beds, *Int. J. Hydrogen Energy*, Vol. 32, Issue 12, pp. 1969–1981.

MacDonald, B. D. and Rowe, A. M. (2006) Impacts of External Heat Transfer Enhancements on Metal Hydride Storage Tanks, *Int. J. Hydrogen Energy*, Vol. 31, Issue 12, pp. 1721–1731.

MacDonald, B. D. and Rowe, A. M. (2007) Experimental and Numerical Analysis of Dynamic Metal Hydride Hydrogen Storage Systems, *J. Power Sources*, Vol. 174, Issue 1, pp. 282–293.

Marty, P., Fourmigue, J., Rango, P. D., Fruchart, D., and Charbonnier, J. (2006) Numerical Simulation of Heat and Mass Transfer during the Absorption of Hydrogen in a Magnesium Hydride, *Energy Conversion Management*, Vol. 47, Issue 20, pp. 3632-3643.

Mat, M. D. and Kaplan, Y. (2001) Numerical Study of Hydrogen Absorption in an Lm-Ni5 Hydride Reactor, *Int. J. Hydrogen Energy*, Vol. 26, Issue 9, pp. 957–963.

Mat, M. D., Kaplan, Y., and Aldas, K. (2002) Investigation of Three-Dimensional Heat and Mass Transfer in a Metal Hydride Reactor, *Int. J. Energy Res.*, Vol. 26, Issue 11, pp. 973–986.

Mayer, U., Groll, M., and Supper, W. (1986) Heat and Mass Transfer in Metal Hydride Reaction Beds: Experimental and Theoretical Results, *J. Less-Common Metals*, Vol. 131, pp. 235–244.

Moran, M. J. and Shapiro, H. N. (2004) *Fundamentals of Engineering Thermodynamics*, 5th ed., John Wiley & Sons, Hoboken, NJ.

Nakagawa, T., Inomata, A., Aoki, H., and Miura, T. (2000) Numerical Analysis of Heat and Mass Transfer Characteristics in the Metal Hydride Bed, *Int. J. Hydrogen Energy*, Vol. 25, Issue 4, pp. 339–350.

Nakamura, Y., Oguro, K., Uehara, I., and Akiba, E. (2000) X-Ray Diffraction Peak Broadening and Degradation in LaNi5-Based Alloys, *Int. J. Hydrogen Energy*, Vol. 25, Issue 6, pp. 531–537.

NIST Chemistry WebBook (2007) Isothermal Properties for Hydrogen, http://webbook.nist.gov/chemistry /fluid/, last accessed June 2007.

Oi, T., Maki, K., and Sakaki, Y. (2004). Heat Transfer Characteristics of the Metal Hydride Vessel Based on the Plate-Fin Type Heat Exchanger, *J. Power Sources*, Vol. 125, Issue 1, pp. 52–61.

Sastri, M. V. C., Viswanathan, B., and Murthy, S. S. (1998) *Metal Hydrides: Fundamentals and Applications*, Springer-Verlag, New York.

Schlapbach, L., Bowman, R. C., Gerard, N., and Lotsch, H. (1992) *Hydrogen in Intermetallic Compounds II: Surface and Dynamic Properties*, Applications, Springer-Verlag, Berlin.

Sun, D. and Deng, S. (1988) Study of the Heat and Mass Transfer Characteristics of Metal Hydride Beds, *J. Less-Common Metals*, Vol. 141, Issue 1, pp. 37–43.

Sun, D. and Deng, S. (1989) Study of the Heat and Mass Transfer Characteristics of Metal Hydride Beds. A Two-Dimensional Model, *J. Less-Common Metals*, Vol. 155, Issue 2, pp. 271–279.

Takeichi, N., Senoh, H., Yokota, T., Tsuruta, H., Hamada, K., Takeshita, H. T., Tanaka, H., Kiyobayashi, T., Takano, T., and Kuriyama, N. (2003) "Hybrid Hydrogen Storage Vessel", a Novel High-Pressure Hydrogen Storage Vessel Combined with Hydrogen Storage Material, *Int. J. Hydrogen Energy*, Vol. 28, Issue 10, pp. 1121–1129.

Toh, K., Kubo, H., Isogai, Y., Mori, D., Hirose, K., and Kobayashi, N. (2006) Thermal Analysis of High-Pressure Metal Hydride Tank for Automo-

tive Application, *Mater. Res. Soc. Symp. Proc.*, Vol. 927, pp. 1–8.

Vargaftik, N. B. (1975) *Tables on the Thermophysical Properties of Liquids and Gases: In Normal and Dissociated States*, 2nd ed., Hemisphere Pub. Corp., Washington.

Zhang, J., Fisher, T. S., Ramachandran, P. V., Gore, J. P., and Mudawar, I. (2005) A Review of Heat Transfer Issues in Hydrogen Storage Technologies, *J. Heat Transfer*, Vol. 127, Issue 12, pp. 1391–1399.

Zheng, Y., Velagapudi, V., Pourpoint, T., Fisher, T. S., Mudawar, I., and Gore, J. P. (2006) Thermal Management Analysis of On-Board High-Pressure Metal Hydride Systems, *2006 ASME Int. Mechanical Engineering Congress and Exposition*, Chicago, Illinois, USA, Paper No. 14080.